JOURNAL OF AGRICULTURAL AND FOOD CHEMISTRY

Article

pubs.acs.org/JAFC

Unraveling the Chemical Composition of Caramel

Agnieszka Golon and Nikolai Kuhnert*

School of Engineering and Science, Jacobs University Bremen, 28759 Bremen, Germany

Supporting Information

ABSTRACT: Caramel is one of mankind's best known dietary materials obtained from carbohydrates by heating. Much effort has been expended toward the chemical characterization of the components of caramel but impeded by a lack of suitable analytical techniques sufficiently powerful for providing insight into an extraordinarily complex material. This paper reports the characterization of caramel formed by heating from glucose, fructose, and saccharose using a conceptually novel combination of mass spectrometrical techniques. The analytical strategy employed uses high-resolution mass spectrometry (MS) followed by targeted liquid chromatography−tandem MS experiments. Caramel is composed from several thousand compounds formed by a small number of unselective and chemoselective reactions. Caramelization products include oligomers with up to six carbohydrate units formed through unselective glycosidic bond formation, dehydration products of oligomers losing up to a maximum of eight water molecules, hydration products of sugar oligomers, disproportionation products, and colored aromatic products.

KEYWORDS: *carbohydrates, monosaccharides, disaccharides, browning, caramel, Maillard reaction, mass spectrometry, complex mixtures*

INTRODUCTION

Watching white crystalline sugar turn into brown caramel, producing an enticing and appetizing aroma, must be one of the first childhood exposures to chemistry for most humans. Caramel constitutes one of mankind's oldest and most important dietary materials produced and consumed at an estimated level of 50 Mt per annum.[1] Despite its high profile, the chemical composition of the reaction products of heated sugar remains until the present day largely elusive if not mysterious.[2]

Although much effort has been expended toward the investigation of the volatile compounds formed in caramelization, the chemistry and structure of the nonvolatile components of caramel have been investigated on only a few occasions with little structural insight provided, due to the extraordinary chemical complexity of caramel samples. Within the volatile fraction of caramel, diacetyl,[3] associated with a butterscotch type flavor, is one of the best characterized aroma compounds in caramel, which is accompanied by several hundreds of other flavor compounds identified, in particular, furans, produced after dehydration of carbohydrates, such as hydroxymethylfurfural (HMF) and hydroxyacetylfuran (HAF); furanones, such as hydroxydimethylfuranone (HDF), dihydroxydimethylfuranone (DDF), and maltol from disaccharides; and hydroxymaltol, from monosaccharides.[4,5]

Within the nonvolatile fraction, caramelization yields several ill-defined products with fructose dianhydride, being one of the few well-characterized reaction products that were described.[6−13] In 1967 Kitaoka classified the reaction products of caramelization into three distinct classes: caramelans, tetramers of hexoses ($C_{24}H_{36}O_{18}$); caramelens, hexamers of glucose ($C_{36}H_{50}O_{25}$); and caramelins, polymers of glucose ($C_{125}H_{188}O_{80}$).[14,15] Although this classification is reported frequently, with an added hint that caramelization is accompanied by loss of water from carbohydrates, this early classification has never attracted the attention of other research groups or has never been further substantiated, impeded by the lack of sufficiently powerful analytical methods able to unravel the complexity of the product mixture formed in caramelization.

The aim of this contribution is to give a comprehensive account of the chemical structures of the reaction products formed when glucose **1**, fructose **2**, or saccharose **3**, the three most relevant dietary carbohydrates, are heated to form brown caramel. The characterization approach taken uses a conceptually novel combination of modern mass spectrometry techniques. We employ here for the first time for a complex dietary material high-resolution mass spectrometry (MS) and liquid chromatography−tandem mass spectrometry (LC-MS) together with recently developed data interpretation strategies to provide information at a level corresponding technically to the state of the art of analytical chemistry. This approach combines the best of three worlds: ultimate resolution, high sensitivity, and selectivity through targeted ion monitoring. Obvious limitations of the approach exist, considering that thousands of reaction products are formed that can physically be neither separated nor compared to authentic reference materials.[16] Our analytical strategy employs both high-resolution MS measurements as direct infusions and LC-MS measurements to generate molecular formula lists. Parameters extracted from these lists are subjected to graphical interpretation tools such as the van Krevelen analysis, homologous series analysis, and Kendrick analysis to provide a rough picture about structural trends, likely reaction mechanisms, and inspiration for a structural hypothesis.[16] The resulting structural hypothesis was then subjected to further scrutiny, exploiting the ion selectivity of targeted

Received: November 22, 2011
Revised: January 30, 2012
Accepted: March 1, 2012
Published: March 1, 2012

tandem LC-MS and direct infusion tandem MS experiments, ultimately providing a confirmation of the chemical composition of caramel for selected structures.[17]

MATERIALS AND METHODS

Chemicals. All solvents (analytical grade) and chemicals were purchased from Sigma-Aldrich (Bremen, Germany).

Sample Preparation. All sugar samples (1 g) were heated in an oven for 2 h at 140 °C in the case of fructose and at 180 °C for glucose and saccharose. The caramelized samples were stored at room temperature. Caramelized carbohydrates (1 mg) were dissolved in methanol/water (1:1, v/v, 1 mL) and used directly for micrOTOF and direct infusion ion trap MS. When was required, it was dissolved in water, and used for LC-MS and LC-TOF.

High-Resolution ESI-TOF-MS. High-resolution mass spectra were recorded using a Bruker Daltonics micrOTOF Focus instrument from 1 mg/mL 1:1 methanol/water solutions using the negative and positive electrospray ionization mode. The micrOTOF Focus mass spectrometer (Bruker Daltonics, Bremen, Germany) was fitted with an ESI source. Internal calibration was achieved with 10 mL of 0.1 M sodium formate solution. Calibration was carried out using the enhanced quadratic calibration mode. Samples were infused at a flow rate of 200 μL/h using a syringe pump. All MS measurements were carried out in negative and positive ion modes.

HPLC. Separation was achieved on a 250 × 4.6 mm i.d. column containing diphenyl, 5 μm, and a 5 × 4.6 mm i.d. guard column of the same material (Varian, Darmstadt, Germany). Solvent was water/formic acid (1000:0.05 v/v). Solvent was delivered at a total flow rate of 850 μL/min by 25 min isocratic.

LC-MS^n. The LC equipment (Agilent 1100 series, Bremen, Germany) comprised a binary pump, an autosampler with a 100 μL loop, and a diode array detector with a light-pipe flow cell (recording at 320 and 254 nm and scanning from 200 to 600 nm). This was interfaced with an ion trap mass spectrometer fitted with an ESI source (Bruker Daltonics HCT Ultra) operating in Auto MS^n mode to obtain fragment ion m/z. As necessary, MS^2, MS^3, and MS^4 fragment-targeted experiments were performed to focus only on compounds producing a parent ion at m/z 143, 161, 179, 197, 287, 305, 323, 341, 359, 449, 431, 467, 485, 503, 521, 611, 629, 647, 665, 683, 773, 791, 809, 827, and 845. Tandem mass spectra were acquired in Auto-MS^n mode (smart fragmentation) using a ramping of the collision energy. Maximum fragmentation amplitude was set to 1 V, starting at 30% and ending at 200%. MS operating conditions (negative mode) had been optimized using glucose with a capillary temperature of 365 °C, a dry gas flow rate of 10 L/min, and a nebulizer pressure of 12 psi.

LC-TOF-MS. High-resolution LC-MS experiments were carried out using the same HPLC equipped with a micrOTOF Focus mass spectrometer (Bruker Daltonics) fitted with an ESI source. An internal calibration was achieved with 10 mL of 0.1 M sodium formate solution injected through a six-port valve prior to each chromatographic run. Calibration was carried out using the enhanced quadratic calibration mode.

Thermogravimetric Analysis (TGA). NMR, IR, and MALDI-TOF experimental procedures are given in the Supporting Information.

RESULTS AND DISCUSSION

First, we needed to decide on a protocol to obtain caramel. A differential TGA of glucose and saccharose revealed that 2 h of reaction time at 180 °C (for fructose, 140 °C) is required to induce a weight loss of 10−12%. This weight loss corresponds statistically to the loss of one water molecule per carbohydrate monomer and would correspond to a completion of reaction. This observation was substantiated by monitoring the starting material concentration over time, indicating that after 2 h of reaction time at 180 °C around 5% of the initial monomeric carbohydrate was present as judged by the intensity of the ion at m/z 179.1 for glucose and fructose and at m/z 341.2 for saccharose in negative ion mode.

Second, we needed to decide on the resolving power of the mass spectrometer used. Reemtsma and Hertkorn[18] have recently argued that in order to resolve a complex mixture containing compounds with an elemental composition of CHO only, a resolution of around 20000 at m/z 300, corresponding to the specifications of a time-of-flight (TOF) instrument, should be sufficient to resolve all theoretically possible isobaric ions of a mass below m/z 800. In recent work on black tea thearubigin natural material with CHO composition, we could confirm this prediction, with TOF-MS and FT-ICR-MS measurements leading to similar levels of resolution and molecular formula assignment results.[19] Hence, we started our investigation by acquiring ESI-TOF-MS data of direct infusion of caramelization products obtained after heating glucose and saccharose for 2 h at 180 °C and fructose at 140 °C. Depending on the signal-to-noise ratio chosen, the spectra revealed several hundred to several thousand signals (due to the page restriction we limit the analysis and discussion to a S/N ratio of 500 with around 300 signals detected in the samples) in a m/z range between 50 and 1200, with no signals present above this value. Typical mass spectra for glucose caramelization are shown in Figure 1.

Using MALDI-TOF mass spectrometry with 2,5-dihydroxybenzoic acid (DHB) as a matrix, additional oligomeric hexoses at m/z 1499.61, 1661.58, and 1805.62 corresponding to nonamers, decamers, and undecamers could be observed, similar to degradation products of coffee carbohydrates reported recently by the group of Coimbra.[20]

The number of distinct compounds in caramel is therefore a minimum of number of compounds (around 300) detected in direct infusion ESI-MS multiplied by the number of potential isomers corresponding to each ion. Generation of molecular formulas from these data provided mass lists, which were subjected to peak assignment and several graphical interpretation tools.

Assignment of the 40 most intense peaks for the glucose sample is shown in Table 1 (assignments for fructose and saccharose are given in the Supporting Information).

Van Krevelen diagrams were generated that display in a two-dimensional plot each data point as a pair of elemental ratios H/C and O/C.[21] This type of plot allows two conclusions. First, each class of chemical compound can be defined by elemental ratio boundaries, for example, carbohydrates with a H/C ratio around 2 and an O/C ratio of around 1. Second, with the elemental ratio of the starting material known, reaction types that alter this elemental composition can be identified. The van Krevelen diagrams for glucose, fructose, and saccharose are shown in Figure 2. The following information can be extracted from these diagrams: (1) Data points with characteristic carbohydrate elemental ratios exist in the sample (top right corner labeled I). (2) Data points on a diagonal line with negative slope indicate successive loss of water along a series of different reaction products (labeled II). (3) Data points on the left top corner indicate formal reduction (a loss of oxygen content), which seems to be compensated by further reaction products gaining oxygen, overall leading to redox disproportionation (labeled III). (4) Data points in the bottom left of the plot indicate the formation of aromatic compounds (labeled IV).

Next, a homologous series analysis was carried out. This interpretation tool allows the extraction of homologous series

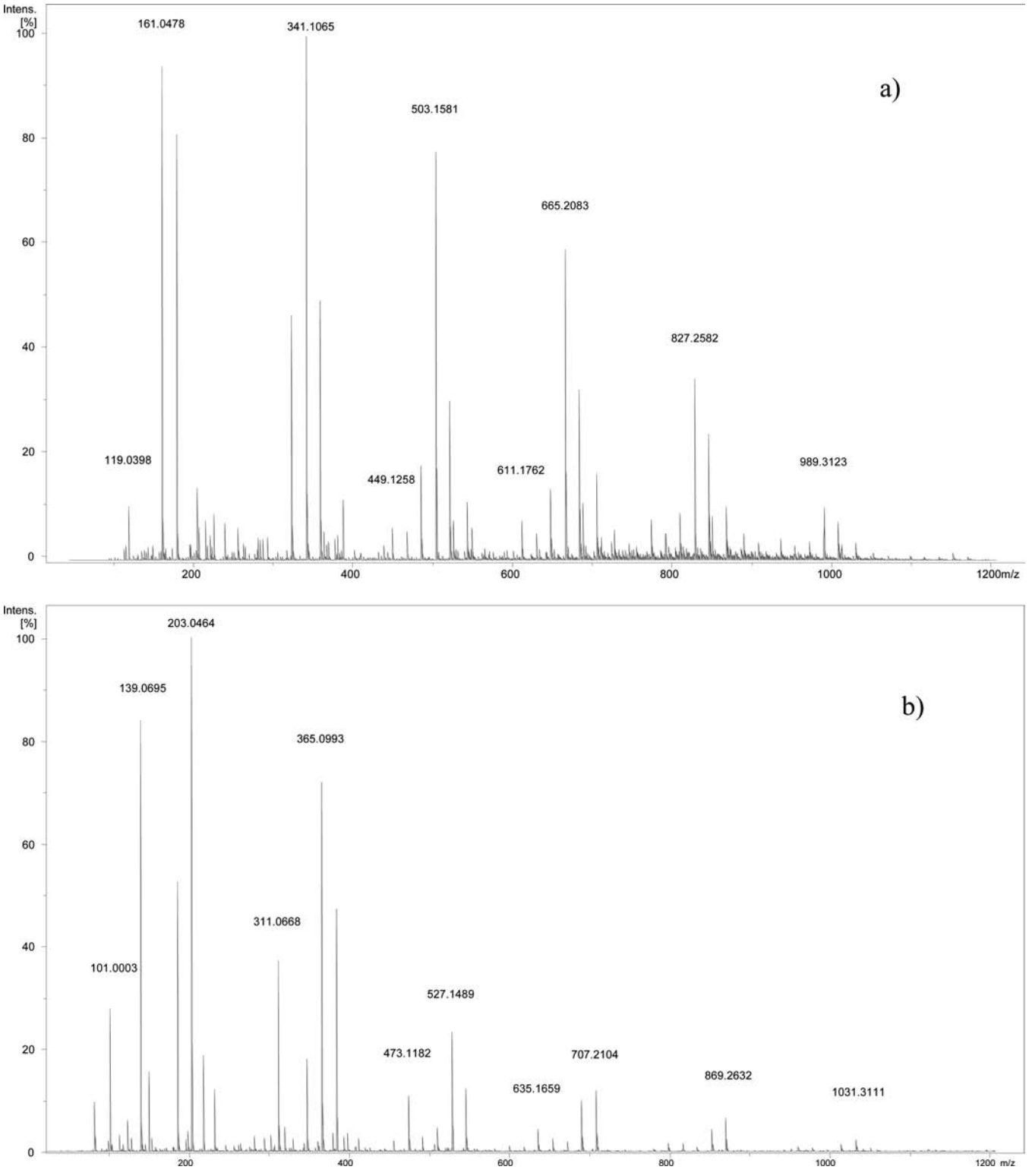

Figure 1. Direct infusion mass spectra of caramelized glucose (a) in the negative ion mode and (b) in the positive ion mode using a direct infusion into an ESI-TOF-MS instrument.

of compounds, meaning series of compounds that differ by defined mass increments, to identify both series and the increment.[19] Such an analysis reveals that mass increments of $-H_2O$, $+C_6H_{10}O_5$, $+C_6H_8O_4$, and $C_6H_6O_3$ are most commonly encountered in the samples corresponding to addition and loss of water, addition of a monosaccharide, and addition of a dehydrated monosaccharide. To verify such mass increments within the original data set, a Kendrick analysis or mass defect analysis was carried out, using the above mass increments as normalization parameters.[22] A Kendrick plot normalized to H_2O of glucose is shown in Figure 3 (those for fructose and saccharose are given in the Supporting Information). From these diagrams it becomes immediately obvious that several homologous series of compounds exists, which beginning from

dx.doi.org/10.1021/jf204807z | J. Agric. Food Chem. 2012, 60, 3266–3274

Table 1. High-Resolution Mass (MS-TOF) Data for Caramelized Glucose in the Negative Ion Mode

			m/z [M − H]		
peak	assignment	mol formula	exptl	theor	relative error (ppm)
1		$C_6H_{12}O_2$	115.0762	115.0765	2.3
2		$C_4H_8O_4$	119.0347	119.0350	2.6
3		$C_8H_8O_2$	135.0452	135.0452	0.4
4		$C_8H_{16}O_2$	143.1075	143.1078	2.0
5		$C_9H_{18}O_2$	157.1232	157.1234	1.6
6	Glu − H_2O	$C_6H_{10}O_5$	161.0452	161.0455	2.2
7	glucose	$C_6H_{12}O_6$	179.0563	179.0561	0.9
8		$C_7H_{14}O_8$	225.0610	225.0616	2.7
9		$C_{16}H_{32}O_2$	255.2320	255.2330	3.7
10		$C_{15}H_{22}O_4$	265.1442	265.1445	1.1
11		$C_9H_{18}O_9$	269.0875	269.0878	1.2
12		$C_{18}H_{36}O_2$	283.2646	283.2643	1.3
13	$(Glu)_2$ − 3 × H_2O	$C_{12}H_{16}O_8$	287.0776	287.0772	1.1
14		$C_{17}H_{26}O_4$	293.1761	293.1758	1.0
15	$(Glu)_2$ − 2 × H_2O	$C_{12}H_{18}O_9$	305.0869	305.0878	2.8
16	$(Glu)_2$ − H_2O	$C_{12}H_{20}O_{10}$	323.0998	323.0984	4.4
17	$(Glu)_2$	$C_{12}H_{22}O_{11}$	341.1076	341.1089	3.8
18	$(Glu)_2$ + H_2O	$C_{12}H_{24}O_{12}$	359.1194	359.1195	0.2
19	$(Glu)_3$ − 4 × H_2O	$C_{18}H_{24}O_{12}$	431.1187	431.1195	1.7
20	$(Glu)_3$ − 3 × H_2O	$C_{18}H_{26}O_{13}$	449.1308	449.1301	1.6
21	$(Glu)_3$ − 2 × H_2O	$C_{18}H_{28}O_{14}$	467.1412	467.1406	1.2
22	$(Glu)_3$ − H_2O	$C_{18}H_{30}O_{15}$	485.1526	485.1512	1.2
23	$(Glu)_3$	$C_{18}H_{32}O_{16}$	503.1607	503.1618	2.0
24	$(Glu)_3$ + H_2O	$C_{18}H_{34}O_{17}$	521.1718	521.1723	1.0
25	$(Glu)_4$ − 3 × H_2O	$C_{24}H_{36}O_{18}$	611.1853	611.1829	3.9
26	$(Glu)_4$ − 2 × H_2O	$C_{24}H_{38}O_{19}$	629.1961	629.1935	4.3
27	$(Glu)_4$ − H_2O	$C_{24}H_{40}O_{20}$	647.2037	647.2040	0.5
28	$(Glu)_4$	$C_{24}H_{42}O_{21}$	665.2115	665.2146	4.6
29	$(Glu)_4$ + H_2O	$C_{24}H_{44}O_{22}$	683.2278	683.2251	4.0
30	$(Glu)_5$ − 4 × H_2O	$C_{30}H_{44}O_{22}$	755.2242	755.2251	1.2
31	$(Glu)_5$ − 3 × H_2O	$C_{30}H_{46}O_{23}$	773.2391	773.2357	4.4
32	$(Glu)_5$ − 2 × H_2O	$C_{30}H_{48}O_{24}$	791.2494	791.2463	3.9
33	$(Glu)_5$ − H_2O	$C_{30}H_{50}O_{25}$	809.2565	809.2568	0.4
34	$(Glu)_5$	$C_{30}H_{52}O_{26}$	827.2709	827.2674	4.2
35	$(Glu)_5$ + H_2O	$C_{30}H_{54}O_{27}$	845.2821	845.2780	4.9
36	$(Glu)_6$ − 3 × H_2O	$C_{36}H_{56}O_{28}$	935.2874	935.2885	1.2
37	$(Glu)_6$ − 2 × H_2O	$C_{36}H_{58}O_{29}$	953.3027	953.2991	3.7
38	$(Glu)_6$ − H_2O	$C_{36}H_{60}O_{30}$	971.3109	971.3097	1.3
39	$(Glu)_6$	$C_{36}H_{62}O_{31}$	989.3230	989.3202	2.8

starting materials of different masses lose several molecules of water (up to eight), identified as data points on lines parallel to the *x*-axis on the Kendrick plot.

From manual inspection of the mass spectra and these type of analysis, the following structural hypotheses were drawn regarding the products formed in the caramelization reaction. (i) Oligomers of the starting materials are present with up to a maximum of six monomeric hexoses. (ii) Dehydration products of both monomeric hexoses and oligomeric hexoses are present in the samples, showing successive loss of up to eight water molecules depending on the number of monomers. Pseudomolecular ions corresponding to loss of one and three waters are most abundant and show the MS highest intensity. (iii) Hydration products are present in the sample with up to two water molecules added to an oligomeric carbohydrate. (iv) Fragmentation products arising from a redox disproportionation reaction are present as minor components at an overall reduced and increased oxidation level. (v) Minor aromatic compounds obtained through excessive dehydration are present.

The chemical nature of these reaction products now requires further investigation by liquid chromatography coupled to tandem mass spectrometry. This approach allows isomer separation by LC concomitant with selective ion monitoring of selected classes of compounds. In the following section, data for glucose caramelization, as representative example, are discussed in detail, and discussions and data on fructose and saccharose are presented in the Supporting Information.

Oligomers of Hexose. Both the ESI-TOF-LC-MS direct infusion measurements and ESI-TOF-LC-MS measurements revealed the presence of oligomers of hexoses **4** formed from glucose with a maximum number of six hexoses incorporated at m/z values of 179.1 (glucose), 341.1 ($C_{12}H_{22}O_{11}$), 503.2 ($C_{18}H_{32}O_{16}$), 665.2 ($C_{24}H_{42}O_{21}$), 827.3 ($C_{30}H_{52}O_{26}$), and 989.3 ($C_{36}H_{62}O_{31}$) in the negative ion mode (Figure 4) and sodiated pseudomolecular ions in the positive ion mode at 203.1 (glucose), 365.1 ($C_{12}H_{22}O_{11}$), 527.2 ($C_{18}H_{32}O_{16}$), 689.2

dx.doi.org/10.1021/jf204807z | J. Agric. Food Chem. 2012, 60, 3266−3274

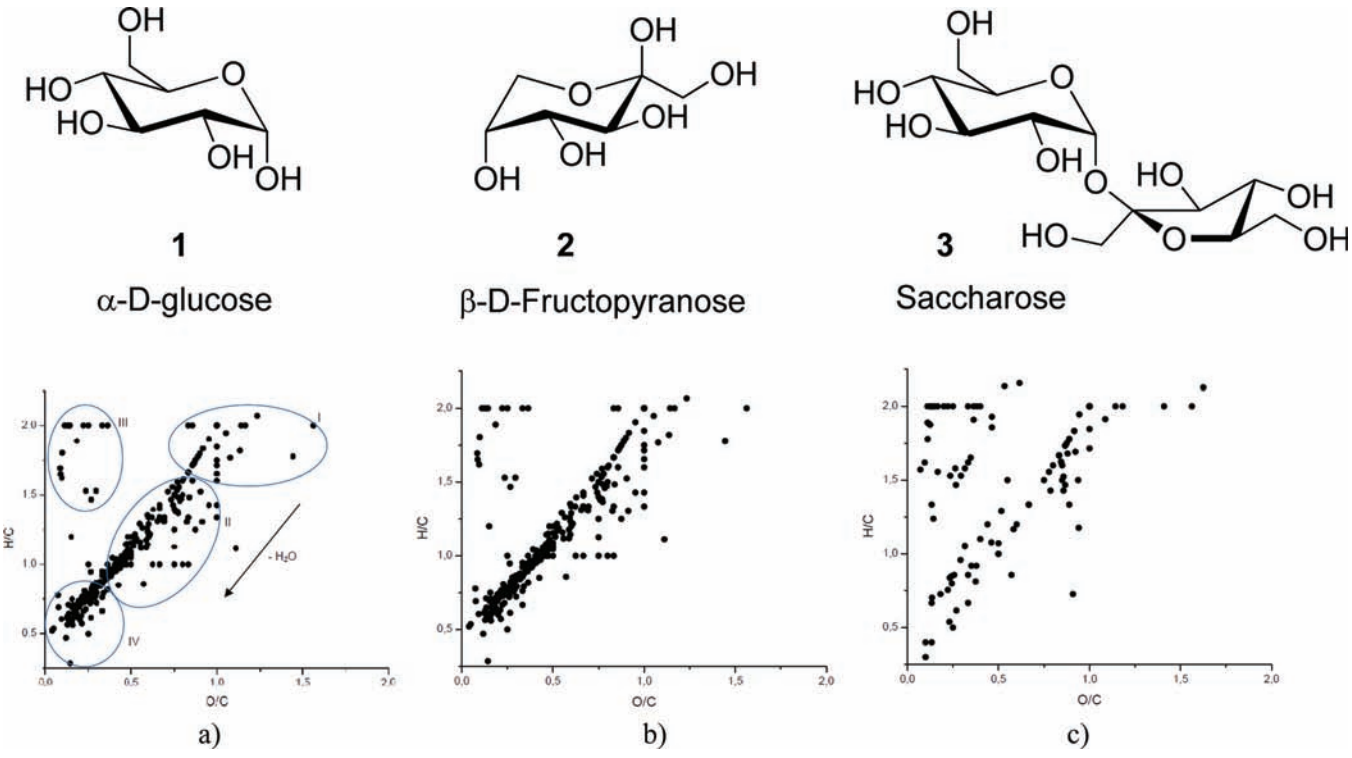

Figure 2. Two-dimensional van Krevelen plot (elemental ratio plot) showing the O/C ratio versus H/C ratio of (a) 284 signals with a S/N ratio of 20 for caramelized glucose, (b) 113 signals with a S/N ratio of 20 for caramelized fructose, and (c) 158 signals with a S/N ratio of 20 for caramelized saccharose in the negative ion mode in the m/z range between 50 and 1200.

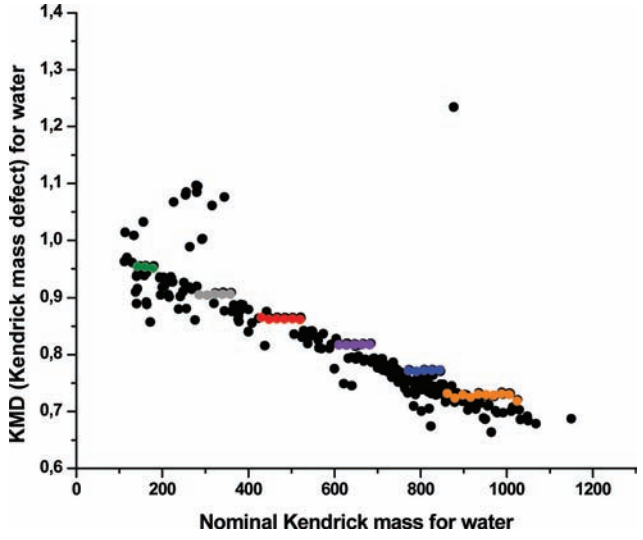

Figure 3. Two-dimensional Kendrick plot for mass increment H_2O showing the distribution of the Kendrick mass defect plotted against the nominal Kendrick mass of pseudomolecular ions for glucose in the negative ion mode. Colored data points parallel to the x-axis indicate homologous dehydration series.

($C_{24}H_{42}O_{21}$), 851.3 ($C_{30}H_{52}O_{26}$), and 913.3 ($C_{36}H_{62}O_{31}$). Targeted tandem-LC-MS measurements at m/z values of 179.1, 341.1, 503.2, 665.2, 827.3, and 989.3 furnished extracted ion chromatograms (EICs) for the six m/z values corresponding to the oligomeric hexoses. Each EIC showed multiple chromatographic peaks (see the Supporting Information). For example, for the ion at m/z 341.1 corresponding to diglucose, a total of eight resolved chromatographic peaks were observed, one of high, two of medium, and five of low intensity, each displaying an MS^2 spectrum consistent with a dimer of glucose (see Figure 5).[23−25] Some MS^2 spectra were identical, whereas others displayed subtle differences. This finding is consistent with an unselective formation of a glycosidic bond to give 8 of all 20 theoretically possible regio- and stereoisomers of diglucose. An alternative epimerization process rationalizing this finding could be ruled out by control experiments. These control experiments included a comparison of LC-MS data for caramelized glucose with those of caramelized mannose and galactose complemented by a GC-MS analysis of a caramel sample hydrolyzed by acid treatment followed by Me_3SiCl derivatization. A full set of isomeric glucose derivatives with similar tandem MS data for all 10 theoretically possible caffeoyl esters of glucose was reported previously.[26] Similar multiple chromatographic peaks were observed for trimers, tetramers, pentamers, heptamers, and hexamers of glucose,; however, with increasing molecular weight it must be assumed that the complete set of regio- and stereoisomers was not chromatographically resolved.

For saccharose; ions corresponding to oligomers containing three to six hexose units were observed at m/z values of 503.2, 665.2, 827.3, and 989.3. The presence of oligomers with odd numbers of monomeric units is in line with recent observations made from thermochemical data by the group of Schmidt.[27]

Dehydration Products. Van Krevelen and Kendrick analyses revealed the presence of homologous series of dehydration products of each oligomer of glucose formed. For glucose, seven dehydration products obtained from a loss of a single water molecule could be observed in EICs at m/z 161.1 in the negative ion mode. The number of signals can be interpreted as the formation of 7 of the 11 theoretically possible isomers of anhydroglucose (see the Supporting Information). After water elimination from glucose at positions C1−C4,

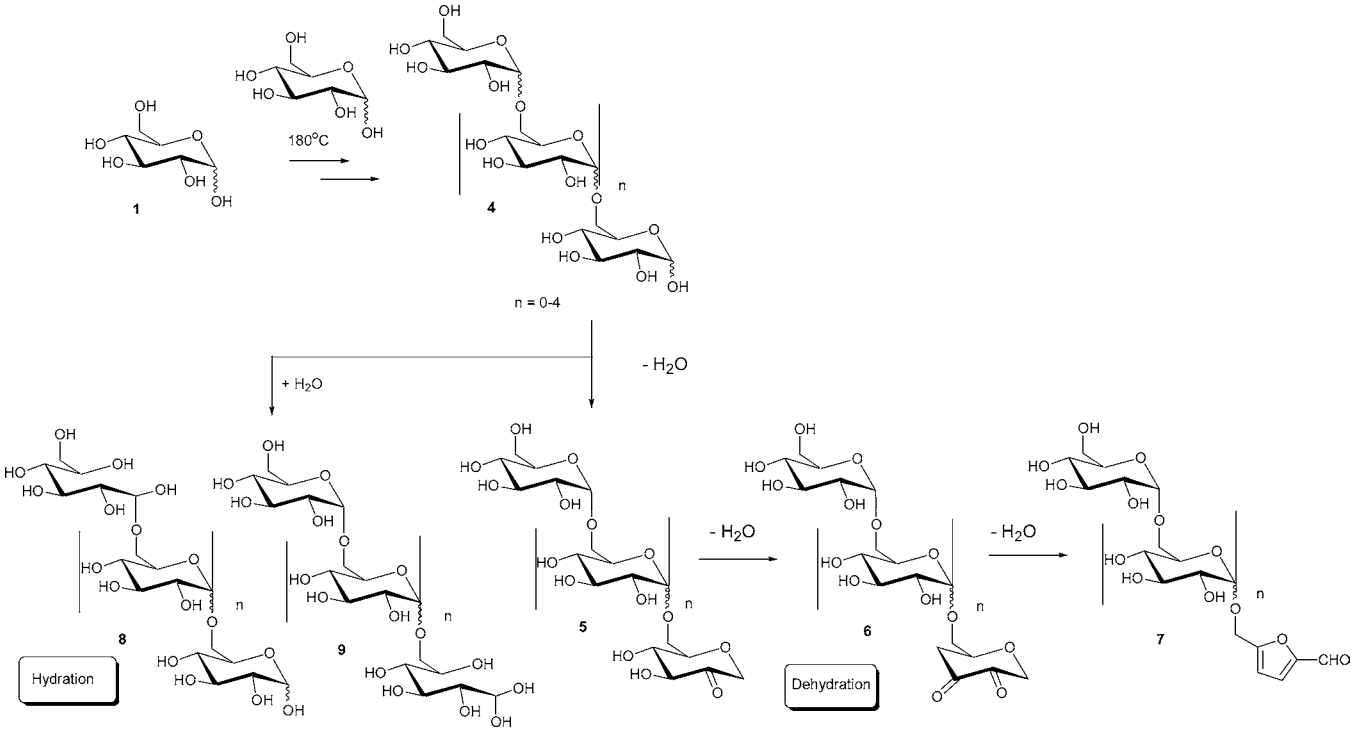

Figure 4. Structures of carbohydrate monomers and potential caramelization products (please note that the regiochemistry of the glycosidic linkage in **4**–**8**, the regiochemistry of dehydration in **5**–**6**, and the regiochemistry of hydrate in **8**, **9** is selected randomly).

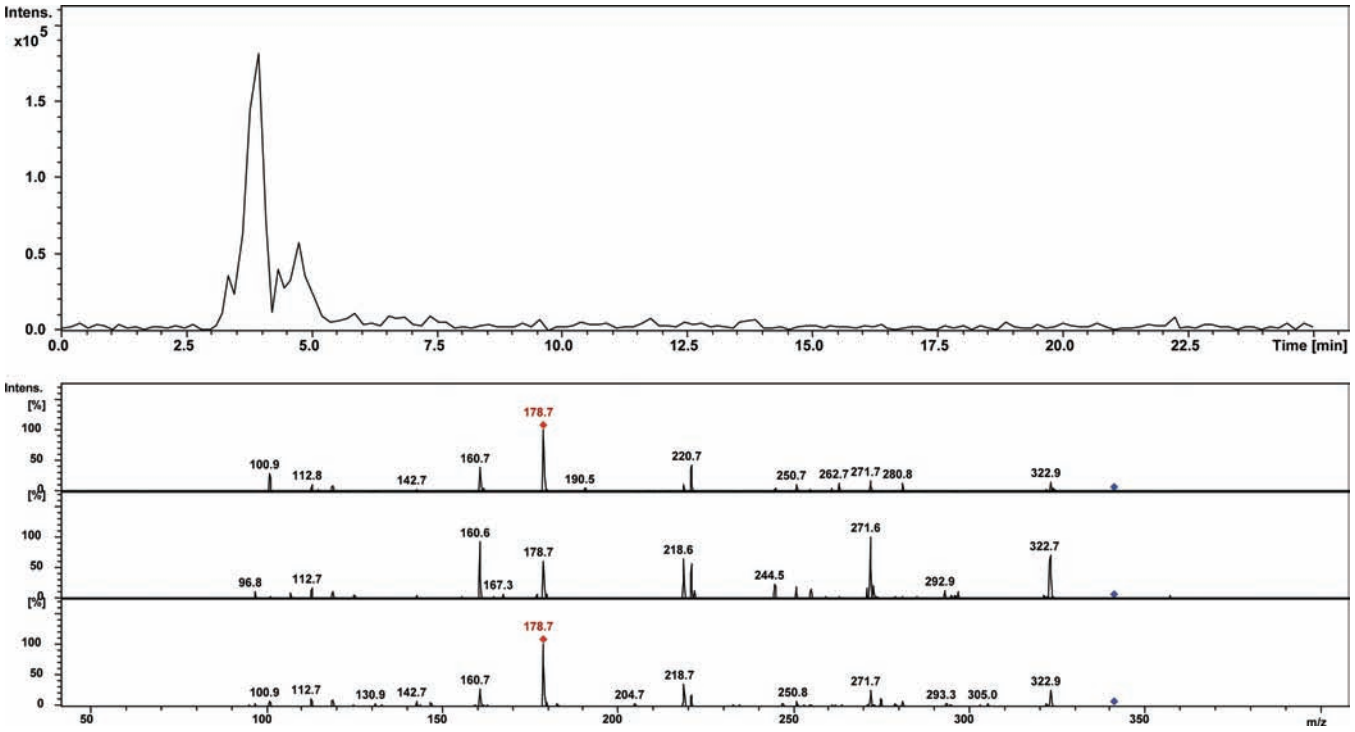

Figure 5. Extracted ion chromatogram (top) and MS^2 spectra (bottom) of pseudomelecular ion at m/z 341.0 ($C_{12}H_{22}O_{11}$) for three selected chromatographic peaks of caramelized glucose in the negative ion mode.

initially an enol is formed that tautomerizes to its ketone form. Evidence for the presence of such ketones is additionally present in both IR and NMR data of the caramel products.

Intense peaks were observed indicating the loss of three water molecules at m/z 287.1, 449.2, 611.2, 773.3, and 935.3 in the negative ion mode and their sodiated adducts at m/z 311.1, 473.2, 635.2, 797.3, and 959.3 in the positive ion mode. MS^2 spectra showed for all compounds the loss of all three waters occurred at the same saccharide moiety with a characteristic neutral loss of −126 ($-C_6H_6O_3$). (For a discussion of fragmentation patterns see the Supporting Information.) These data indicate the formation of a hydroxymethylene

dx.doi.org/10.1021/jf204807z | J. Agric. Food Chem. 2012, 60, 3266–3274

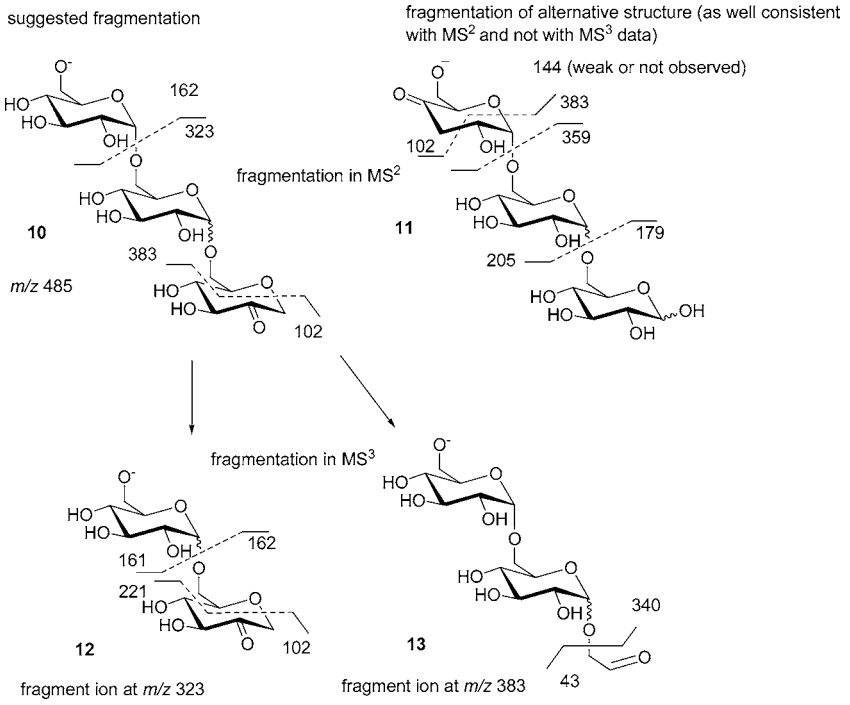

Figure 6. Suggested fragmentation mechanism at m/z 485.1 for the dehydrated ions (regiochemistry of C═O chosen randomly).

furfuraldehyde moiety at the reducing end of the reaction product **7** as suggested by Blank and co-workers in the Maillard reaction of carbohydrates,[29] the presence of which could be further substantiated by characteristic ^{1}H NMR (at 6.5, 7.5, and 9.8 ppm) and ^{13}C NMR shifts of this group (e.g., C═O at 195 ppm) observed in the caramel samples. For oligomers of glucose, dehydration products originating from loss of a single water molecule are observed at m/z 323.1, 485.1, 647.2, and 809.2. In EICs at m/z 323.1 or 485.1 (four peaks each in EICs with one peak of high intensity) were observed. Assuming an E_1 type water elimination in polar liquid caramel, as well suggested by the presence of furfuraldehyde moieties at the reducing end, the main peak observed could be tentatively assigned to the loss of water at the C-1/C-2 position at the reducing end (1-OH terminal glucose moiety), yielding **5**. This assignment is convincingly supported by MS^2 and MS^3 spectra. For example, the main peak at m/z 485.1 **10** or **11** ($Glc_3 - H_2O$, $C_{18}H_{29}O_{15}$) shows a neutral loss of 102 ($-C_4H_6O_3$) in the MS^2 spectrum, which could originate from the loss of a C_4 unit at either the reducing or nonreducing end. Dehydration at the central carbohydrate moiety can be excluded from these data. A further weak peak at m/z 341.1 in MS^2 spectra corresponding to a neutral loss of 144 ($-C_6H_8O_4$) could originate from dehydration at the nonreducing end. Finally, in MS^3 spectra originating from the base peak at m/z 323.1 **12** in MS^2, an intense fragment ion at 83% at m/z 221.1 corresponding to a neutral loss of 102 ($-C_4H_6O_3$) was observed, again rationalized with alternative dehydration from either the reducing end in **10** or the nonreducing terminal carbohydrate moiety in **11**. However, an MS^3 spectra of the fragment ion resulting from a neutral loss of 102 at m/z 383.1 **13** shows two characteristic fragment ions at m/z 340 with a neutral loss of 43 ($-C_2H_3O$) and at m/z 265 with a neutral loss of 118 ($-C_4H_6O_4$), which can be explained only by dehydration at the reducing moiety in tentative structure **13** (see Figure 6).

For both fructose and saccharose intense peaks corresponding to doubly dehydrated at m/z 305 occur, having a fragmentation pattern in line with difructosedianhydride (see the Supporting Information).

Hydration Products. Next to dehydration products, a series of mass spectral signals with molecular formulas corresponding to hydration products of oligosaccharides were observed at m/z 359.2, 521.2, 683.2, 845.3, and 1007.3 (for molecular formulas see Table 1 and for targeted tandem MS data see the Supporting Information). The MS^2 data obtained again from targeted tandem MS experiments are fully consistent with initial hydration at any of the at least two anomeric centers with a neutral loss of 180.1 Da observed from the pseudomolecular ions at m/z 359.2, 521.2, 683.2, 845.3, and 1007.3. Hence, the hydration products were identified as open-chain hemiacetal structures such as **8** and **9** (see Figure 4). Alternatively, a Lobry-de Bruin–Alberda-van Eckenstein isomerization could be envisaged, in which the position of the carbonyl group changes along the carbon backbone followed by water addition to a ketone functionality. The tandem MS data do not allow at this stage clear distinction between these two structural alternatives, with a weak fragment ion at m/z 221 originating from a 359 precursor ion comprising the only intact hydrated fragment ion. Interestingly, water formed in thermal dehydration not only evaporates in caramelization but also acts as a reagent for the chemical modification of caramelization products.[29,30] This represents a phenomenon observed here for the first time.

Redox Disproportionation Products. The van Krevelen plot revealed the presence of a series of minor compounds presumably formed in a redox reaction as "cross peaks" with respect to the dehydration diagonal. Ions with molecular formulas consistent with reduction include, for example, $C_8H_{16}O_2$, $C_{14}H_{28}O_2$, $C_{15}H_{30}O_2$, $C_{18}H_{36}O_2$, $C_{15}H_{22}O_4$, or $C_{17}H_{24}O_4$. Using LC-tandem MS no further structural information could be obtained on these minor compounds; however, similar redox

disproportionations have been suggested by Blank and co-workers while studying the formation of furans in Maillard reactions.[28]

Aromatics and the Colored Compounds in Caramel. Caramel is a material of brown color, and the identity of the coloring compounds is so far unknown, prompting some further investigation. Caramel color produced by base-induced heating of sugar is as well sold as food coloring under the name E150. Van Krevelen diagrams indicated the formation of a series of minor aromatic compounds falling into elemental ratio boundaries of typical aromatic dye molecules. Brown color can originate from two distinct mechanisms: from light scattering with a λ^{-4} dependency in the absorption spectrum, which is not observed here, or, alternatively, brown as a "tertiary color" requires absorption at three distinct wavelengths, of which two must be complementary, as shown to be the case here. Optimized chromatographic conditions using a HPLC gradient with the higher organic solvent percentage required for the identification of lipophilic aromatic chromophores, which were apparent as minor products in van Krevelen plots, revealed, if monitored using UV−vis detection at 400, 450, and 500 nm, a single sharp chromatographic peak at identical retention times for all three wavelengths. This observation suggests that caramel color arises from three distinct chromophoric molecules coeluting or from several close eluting compounds. The mass spectra associated with the chromatographic peak in question showed signals for around 30 coeluting compounds. To identify likely caramel dyes, a van Krevelen plot was produced from high-resolution mass data of this chromatographic peak, which suggested in the typical aromatic region a total of five compounds that would fall within the elemental ratio boundaries expected for an aromatic dye obtained from sugars upon heating with molecular formulas of $C_{24}H_{20}O_{15}$, $C_{32}H_{20}O_4$, $C_{15}H_{12}O_6$, and $C_{20}H_{10}O_4$ (see the Supporting Information for chromatograms and van Krevelen plots). Similar aromatic structures have been proposed in the carbonization of glucose under high pressure in aqueous solution in the production of biofuels by the groups of Li and Antonietti.[31,32]

Interestingly, for fructose up to four well-resolved chromatographic peaks monitored at 550 nm could be observed, indicating that the nature of the brown dyes varies significantly between different sugars.

Caramel is formed upon heating of sugar. Here we characterize the components formed in caramelization, using a three-step conceptually novel mass spectrometry characterization approach applied for the first time to thermally processed food. We have shown that caramel, a challenging and enigmatic material formed from a single pure chemical substance, is transformed thermally into several thousand reaction products, displaying an astonishing level of chemical diversity. These several thousand compounds are shown to be formed by a small number of unselective and chemoselective reactions. Products formed in the caramelization of glucose, fructose, and saccharose include oligomers with up to six carbohydrate units formed through unselective glycosidic bond formation, dehydration products of oligomers losing up to a maximum of eight water molecules, including products of initial dehydration at the reducing end sugar leading to hydroxyfurfural derivatives, hydration products of sugar oligomers, disproportionation products, and colored aromatic products for which molecular formulas could be suggested. Aspects of regio- and stereochemistry of caramelization products remain frequently open. In principle, these aspects can be addressed using tandem mass spectrometry[33] but have not yet been established in the field of carbohydrate chemistry.

Caramel is produced and consumed by humans at a level of several tens of million tons annually. The work provided here, using innovative analytical strategies for complex mixture analysis, provides for the first time a comprehensive account of the chemical composition of one of mankind's oldest, most popular, and most important dietary materials.

■ ASSOCIATED CONTENT

Ⓢ Supporting Information

Additional EICs, MS^2 + MS^3 data of all compounds mentioned in the text, table of high-resolution MS-TOF data for compounds identified, NMR, IR, and MALDI-TOF data. This material is available free of charge via the Internet at http://pubs.acs.org.

■ AUTHOR INFORMATION

Corresponding Author

*Phone: 49 421 200 3120. Fax: 49 421 200 3229. E-mail: n.kuhnert@jacobs-university.de.

Funding

We thank Jacobs University Bremen and the Fond für Angewandte Umweltforschung des Landes Bremen for funding.

Notes

The authors declare no competing financial interest.

■ ACKNOWLEDGMENTS

We acknowledge the technical assistance provided by Anja Müller. We thank one of the referees for pointing out the possibility of a Lobry de Bruin−Alberdavan Eckenstein isomerization.

■ REFERENCES

(1) Davidson, A. *The Oxford Companion to Food*, 3rd ed.; Oxford University Press: Oxford, U.K., 2008.

(2) Kroh, L. W. Caramelisation in food and beverages. *Food Chem.* **1994**, *51*, 373−379.

(3) Luning, P. A.; De Rijk, T.; Wichers, H. J.; Roozen, J. P. Gas Chromatography, mass spectrometry and sniffing port analyses of volatile compounds of fresh bell peppers (*Capsicum annuum*) at different ripening stages. *J. Agric. Food Chem.* **1994**, *42*, 977−983.

(4) Blank, I.; Fay, L. B. Formation of 4-hydroxy-2,5-dimethyl-3(2*H*)-furanone and 4-hydroxy-2(or 5)-ethyl-5(or 2)-methyl-3(2*H*)-furanone through Maillard reaction based on pentose sugars. *J. Agric. Food Chem.* **1996**, *44*, 531−536.

(5) Defaye, J.; Fernández, J. M. G. Protonic and thermal activation of sucrose and the oligosaccharide composition of caramel. *Carbohydr. Res.* **1994**, *256*, C1−C4.

(6) Suarez-Pereira, E.; Rubio, E. M.; Pilard, S.; Mellet, C. O.; Fernández, J. M. G. Di-D-fructose-anhydrides-enriched products by acid ion-exchange resin-promoted caramelization of D-fructose: chemical analyses. *J. Agric. Food Chem.* **2010**, *58*, 1777−1787.

(7) Saito, K.; Tomita, F. Difructose anhydrides: their mass-production and physiological functions. *Biosci., Biotechnol., Biochem.* **2000**, *64*, 1321−1327.

(8) Manley-Harris, M.; Richards, G. N. Di-D-fructose dianhydrides and related oligomers from thermal treatments of inulin and sucrose. *Carbohydr. Res.* **1996**, *287*, 183−202.

(9) Mellet, C. O.; Fernández, J. M. G. Difructose dianhydrides (DFAs) and DFA-enriched products as functional foods. *Top. Curr. Chem.* **2010**, *294*, 49−77.

(10) Christian, T. J.; Manley-Harris, M.; Field, R. J.; Parker, B. A. Kinetics of formation of di-D-fructose dianhydrides during thermal treatment of insulin. *J. Agric. Food Chem.* **2000**, *48*, 1823−1837.

(11) Defaye, J.; Fernández, J. M. G. The oligosaccharide components of caramel. *Zuckerindustrie* **1995**, *120*, 700−704.

(12) Ruiz-Matute, A. I.; Soria, A. C.; Martínez-Castro, I.; Sanz, M. L. A new methodology based on GC-MS to detect honey adulteration with commercial syrups. *J. Agric. Food Chem.* **2007**, *55*, 7264−7269.
(13) Montilla, A.; Ruiz-Matute, A. I.; Sanz, M. L.; Martínez-Castro, I.; Del Castillo, M. D. Difructose anhydrides as quality markers of honey and coffee. *Food Res. Int.* **2006**, *39*, 801−806.
(14) Kitaoka, S.; Suzuki, K. *Agric. Biol. Chem.* **1967**, *31*, 753.
(15) Tomasik, P.; Palasiński, M.; Wiejak, S. The thermal decomposition of carbohydrates. Part I: The decomposition of mono-, di- and oligosaccharides. *Adv. Carbohydr. Chem. Biochem.* **1989**, *47*, 203−278.
(16) Kuhnert, N. Unraveling the structure of the black tea thearubigins. *Arch. Biochem. Biophys.* **2010**, *501*, 37−51.
(17) Kuhnert, N.; Clifford, M. N.; Müller, A. Oxidative cascade reactions yielding polyhydroxy-theaflavins and theacitrins in the formation of black tea thearubigins: evidence by tandem LC-MS. *Food Funct.* **2010**, *1*, 180−199.
(18) Hertkorn, N.; Frommberger, M.; Witt, M.; Koch, B. P.; Schmitt-Kopplin, P.; Perdue, E. M. Natural organic matter and the event horizon of mass spectrometry. *Anal. Chem.* **2008**, *80*, 8908−8919.
(19) Kuhnert, N.; Drynan, J. W.; Obuchowicz, J.; Clifford, M. N.; Witt, M. Mass spectrometric characterization of black tea thearubigins leading to an oxidative cascade hypothesis for thearubigin formation. *Rapid Commun. Mass Spectrom.* **2010**, *24*, 3387−3404.
(20) Moreira, A. S. P.; Coimbra, M. A.; Nunes, F. M.; Simões, J.; Domingues, M. R. M. Evaluation of the effect of roasting on the structure of coffee galactomannans using model oligosaccharides. *J. Agric. Food Chem.* **2011**, *59*, 10078−10087.
(21) Wu, Z.; Rodgers, R. P.; Marshall, A. G. Two- and three-dimensional van Krevelen diagrams: a graphical analysis complementary to the Kendrick mass plot for sorting elemental compositions of complex organic mixtures based on ultrahigh-resolution broadband Fourier transform ion cyclotron resonance mass measurements. *Anal. Chem.* **2004**, *76*, 2511−2516.
(22) Hughey, C. A.; Hendrickson, C. L.; Rodgers, R. P.; Marshall, A. G.; Qian, K. N. Kendrick mass defect spectrum: a compact visual analysis for ultrahigh-resolution broadband mass spectra. *Anal. Chem.* **2001**, *73*, 4676−4681.
(23) Novotny, M. V.; Mechref, Y. New hyphenated methodologies in high-sensitivity glycoprotein analysis. *J. Sep. Sci.* **2005**, *28*, 1956−1968.
(24) March, R. E.; Stadey, C. J. A tandem mass spectrometric study of saccharides at high mass resolution. *Rapid Commun. Mass Spectrom.* **2005**, *19*, 805−812.
(25) Tang, H. X.; Mechref, Y.; Novotny, M. V. Automated interpretation of MS/MS spectra of oligosaccharides. *Bioinformatics* **2005**, *21*, I431−I439.
(26) Jaiswal, R.; Sovdat, T.; Vivan, F.; Kuhnert, N. Profiling and characterization by LC-MS^n of the chlorogenic acids and hydroxycinnamoylshikimate esters in maté (*Ilex paraguariensis*). *J. Agric. Food Chem.* **2010**, *58*, 5471−5484.
(27) Lee, J. W.; Thomas, L. C.; Jerrell, J.; Feng, H.; Cadwallader, K. R.; Schmidt, S. J. Investigation of thermal decomposition as the kinetic process that causes the loss of crystalline structure in sucrose using a chemical analysis approach (part II). *J. Agric. Food Chem.* **2011**, *59* (2), 702−712.
(28) Limacher, A.; Kerler, J.; Davidek, T.; Schmalzried, F.; Blank, I. Formation of furan and methylfuran by Maillard-type reactions in model systems and food. *J. Agric. Food Chem.* **2008**, *56*, 3639−3647.
(29) Jiang, B.; Liu, Y.; Bhandari, B.; Zhou, W. Impact of caramelization on the glass transition temperature of several caramelized sugars. Part I: chemical analyses. *J. Agric. Food Chem.* **2008**, *56*, 5138−5147.
(30) Ratsimba, V.; Fernández, J. M. G.; Defaye, J.; Nigay, H; Voilley, A. Qualitative and quantitative evaluation of mono- and disaccharides in D-fructose, D-glucose and sucrose caramels by gas−liquid chromatography−mass spectrometry Di-D-fructose dianhydrides as tracers of caramel authenticity. *J. Chromatogr., A* **1999**, *844*, 283−293.
(31) Sun, X.; Li, Y. Colloidal carbon spheres and their core/shell structures with noble-metal nanoparticles. *Angew. Chem., Int. Ed.* **2004**, *43*, 597−601.
(32) Titirici, M. M.; Antonietti, M.; Baccile, N. Hydrothermal carbon from biomass: a comparison of the local structure from poly- to monosaccharides and pentoses/hexoses. *Green Chem.* **2008**, *10*, 1204−1212.
(33) Clifford, M. N.; Johnston, K. L.; Knight, S.; Kuhnert, N. Hierarchical scheme for LC-MS^n identification of chlorogenic acids. *J. Agric. Food Chem.* **2003**, *51*, 2900−2911.